

Article

# VMD-KFCM Algorithm for the Fault Diagnosis of Diesel Engine Vibration Signals

Xiaobo Bi <sup>1,2</sup>, Jiansheng Lin <sup>1</sup>, Daijie Tang <sup>1</sup>, Fengrong Bi <sup>1,\*</sup>, Xin Li <sup>1</sup>, Xiao Yang <sup>1</sup>, Teng Ma <sup>1</sup> and Pengfei Shen <sup>1</sup>

<sup>1</sup> State Key Laboratory of Engines, Tianjin University, Tianjin 300072, China; bixiaobo@tju.edu.cn (X.B.); linjsh@tju.edu.cn (J.L.); tjutangdaijie@tju.edu.cn (D.T.); nvh\_lixin@tju.edu.cn (X.L.); yangxiao@tju.edu.cn (X.Y.); mt258@tju.edu.cn (T.M.); shenpengfei@tju.edu.cn (P.S.)

<sup>2</sup> School of Artificial Intelligence, Hebei University of Technology, Tianjin 300401, China

\* Correspondence: fr\_bi@tju.edu.cn; Tel.: +86-022-27407620 (ext. 8002)

Received: 14 November 2019; Accepted: 26 December 2019; Published: 2 January 2020



**Abstract:** Accurate and timely fault diagnosis for the diesel engine is crucial to guarantee it works safely and reliably, and reduces the maintenance costs. A novel diagnosis method based on variational mode decomposition (VMD) and kernel-based fuzzy c-means clustering (KFCM) is proposed in this paper. Firstly, the VMD algorithm is optimized to select the most suitable  $K$  value adaptively. Then KFCM is employed to classify the feature parameters of intrinsic mode functions (IMFs). Through the comparison of many different parameters, the singular value is selected finally because of the good classification effect. In this paper, the diesel engine fault simulation experiment was carried out to simulate various faults including valve clearance fault, fuel supply fault and common rail pressure fault. Each kind of machine fault varies in different degrees. To prove the effectiveness of VMD-KFCM, the proposed method is compared with empirical mode decomposition (EMD)-KFCM, ensemble empirical mode decomposition (EEMD)-KFCM, VMD-back propagation neural network (BPNN), and VMD-deep belief network (DBN). Results show that VMD-KFCM has advantages in accuracy, simplicity, and efficiency. Therefore, the method proposed in this paper can be used for diesel engine fault diagnosis, and has good application prospects.

**Keywords:** diesel engine; fault diagnosis; variational mode decomposition; kernel-based fuzzy c-means clustering; empirical mode decomposition

## 1. Introduction

Diesel engine has been widely used for its excellent power and economic performance. However, the complexities of diesel engines can easily lead to engine failure [1]. Once a part fails, it will inevitably affect the working state of the whole machine resulting in deterioration in power performance or even an accident. If a fault can be diagnosed in advance, and then can be appropriately repaired to avoid further damage. This is the original intention of our research.

During the past few decades, the signal processing method based on vibration signal has received increased attention in the field of fault diagnosis of rotating machinery. Especially in dealing with rolling bearing faults, it has been successfully applied in the past reports, e.g., [2,3]. Fault diagnosis of engine vibration signal is difficult due to the complex structure and precise components [4]. The response generated by components is mixed nonlinearly, which makes it hard to extract the desired fault information from vibration signal. For instance, the cylinder head vibration signal of diesel engine contains abundant response of multiple forces, including in-cylinder combustion impact, intake valve and exhaust valve closure impact, reciprocating inertia force of piston and various random excitation [5].

A proper signal processing algorithm to extract the fault information plays a key role in machine fault diagnosis.

At present, many effective algorithms are used to decompose vibration signals, such as wavelet transform (WT), empirical mode decomposition (EMD) [6], local mean decomposition (LMD) [7], and so on [8,9]. They can decompose signals to a certain extent and obtain intrinsic characteristic functions of the signals. Since EMD has good self-adaptability and high computational efficiency, the improvement and application of EMD-based algorithm emerge in endlessly [10,11]. However, both EMD and LMD use recursive algorithm in principle, which will accumulate errors in envelope calculation during iteration, resulting in mode aliasing phenomenon and end effect [12,13]. These shortcomings will lead to the reduction of the diagnostic accuracy in the pattern recognition process. Huang et al. [14] proposed the ensemble empirical mode decomposition (EEMD) algorithm, which effectively improved the mode aliasing problem, but also brought new problems such as reduced computational efficiency and white noise removal. Bi et al. [15] proposed a novel algorithm, which combining wavelet de-noising algorithm and EMD to detect knock faults of gasoline engines and proved that it can achieve the same effect as EEMD but the calculation speed is faster.

Since Dragomiretskiy and Zosso [16] proposed the variational mode decomposition algorithm in 2014, it has been applied in diverse areas of signal processing, especially in mechanical fault diagnosis [17,18]. VMD was introduced as an alternative to EMD to decompose signals. VMD can improve the mode aliasing and end effect of EMD greatly and be more robust to noise. Zhang et al. [19] set up the rolling bearing fault signal calculating model of different location defect and made a comparison of the bearing defect characteristic extraction performance between VMD and EMD. The result verified that the VMD can accurately extract the principal mode and has better performance than EMD. Similar comparisons have been made in references [20,21] and the same results have been obtained. However, there are many parameters in VMD that need to be set in advance. At present, these parameters do not have accepted selection criteria. Among them, the most important one is the mode number  $K$ , which directly affects the correctness of decomposition. In addition, the quadratic penalty factor  $\alpha$  directly affects decomposition accuracy and has an important influence on the de-noising performance of the algorithm [16]. Some scholars used various evolution algorithms to optimize these two parameters. Zhang et al. [22] used the maximum weighted kurtosis index as the fitness function of grasshopper algorithm to optimize VMD. Wang et al. [23] proposed a multi-objective particle swarm optimization algorithm to optimize  $K$  and  $\alpha$  in VMD. The symbol dynamic entropy and power spectral entropy were selected as fitness functions. Ren et al. [24] used permutation entropy as fitness function of genetic algorithm to optimize  $K$  and  $\alpha$  of VMD and applied the optimized algorithm to fault diagnosis of crankshaft bearings. However, the introduction of evolution algorithms will reduce the computational efficiency of VMD, which makes it hard to optimize the parameters for each signal. A correlation coefficient is a numerical measure meaning a statistical correlation between two signals. It is also applied to the optimization of VMD [25–27]. Sun G et al. [26] proposed an improved VMD algorithm based on the Newton method and used the correlation coefficient between IMF and the original signal as the termination condition. Other scholars [25,27] who use the correlation coefficient to optimize VMD mostly regard it as the standard of removing noise components. In this paper, correlation coefficient is used to optimize VMD to find the stable state of decomposition, and then get the optimized  $K$  value. The details are shown in Section 2.

Pattern recognition methods are usually including supervised learning and unsupervised learning. Supervised learning methods, like the representative support vector machines (SVM) [28] and artificial neural network (ANN) [29], need training data before classification. Chen Z et al. [30] used SVM analyzing feature parameters extracted from noise signals of loader's gearbox by independent component analysis (ICA) to detect faults and got 92.5% recognition rate. Back propagation neural network (BPNN) is mature in theory and performance and is widely used in pattern recognition [31]. However, it is easy to fall into local optimal value and cannot deal with nonlinear problems [32,33]. Hinton proposed the deep belief network (DBN) in 2006, which led to the research upsurge of deep

learning algorithm [34]. Deep learning methods can extract and abstract low-level features to form high-level features, and then discover the distributed feature representation of data. Prasanna et al. [35] compare the diagnostic accuracy of DBN with the other four fault diagnosis methods including SVM, BPNN, self-organizing maps, and Mahalanobis distance for four engineering classification problems and found that DBN has obvious superiority. Deep learning methods can be well applied in data classification. However, SVM, BPNN, and DBN all need a long training time, which is inefficient and not suitable for massive data processing [36].

For unsupervised learning methods, clustering analysis such as k-means and fuzzy C-means (FCM) is widely used in fault diagnosis because of its efficiency [37,38]. Kernel-based fuzzy C-means clustering (KFCM) [39] is an advanced method that introduces kernel functions to the original FCM algorithm. KFCM has better performance in a nonlinear problem and has been widely applied in image segmentation and fault diagnosis [40,41]. Liu et al. used Gaussian KFCM to analyze eigenvectors compared of normalized photovoltaic voltage, normalized photovoltaic current and fill factor, and realized single faults and compound fault conditions diagnosing [42]. Unsupervised learning method without data training is more suitable for real-time fault diagnosis of diesel engine. In this paper, KFCM is used as the fault classification method after decomposition of VMD. However, the classification accuracy of KFCM is closely related to the input feature vectors. Therefore, appropriate selection of feature vectors is also the focus of later research.

The remainder of the paper is organized as followed. The second section gives a brief overview of the VMD and KFCM algorithms. Then the optimized-VMD method is introduced. The decomposition results of simulation signals by the optimized-VMD and other algorithms are compared. The third section describes the experiments conducted to collect various faulty vibration signals of a certain diesel engine. The fourth section presents the principle of the VMD-KFCM joint method and reports the classification results of the proposed algorithm for the experimental signals and compares it with the other methods. Finally, conclusions are given in the fifth section.

## 2. Theories

### 2.1. Variational Mode Decomposition

Variational mode decomposition is based on the Wiener filter, one-dimensional Hilbert transform, and variational method. The VMD can decompose any real time series signal  $f$  into  $K$  discrete number modes  $u_k(t)$  or called intrinsic mode function (IMF) [16], where each mode is mostly compact around a center frequency  $\omega_k$ , and satisfies that the sum of all modes equals  $f$ . The bandwidth of each mode is estimated through the  $L^2$  norm of the gradient. Details of the VMD algorithm can be found in ref. [16]. In order to search for  $u_k(t)$  and  $\omega_k$ , VMD is required to solve the constrained variational problem as follows:

$$\begin{cases} \min_{\{u_k, \omega_k\}} \left\{ \sum_k \left\| \partial_t \left[ \left( \delta(t) + \frac{j}{\pi t} \right) * u_k(t) \right] e^{-j\omega_k t} \right\|_2^2 \right\} \\ \text{s.t. } \sum_k u_k = f \end{cases} \quad (1)$$

where  $t$  is the time,  $\delta(t)$  is the Dirac distribution,  $*$  represents convolution symbol, and  $\{\omega_k\} = \{\omega_1, \omega_2, \dots, \omega_k\}$  indicates each center frequency.

The penalty parameter  $\alpha$  and the Lagrange multiplication operation  $\lambda(t)$  are introduced to convert the constrained variational problem to non-constrained problem. The  $\alpha$  can guarantee the accuracy of reconstructed signal in the presence of Gaussian noise and the  $\lambda(t)$  can keep the strict enforcement of constraint. Then the augmented Lagrangian is described as below:

$$L(\{u_k, \omega_k\}, \lambda) := \alpha \sum_k \left\| \partial_t \left[ \left( \delta(t) + \frac{j}{\pi t} \right) * u_k(t) \right] e^{-j\omega_k t} \right\|_2^2 + \left\| f(t) - \sum_k u_k(t) \right\|_2^2 + \left\langle \lambda(t), f(t) - \sum_k u_k(t) \right\rangle \quad (2)$$

To solve this equation, the alternate direction method of multipliers (ADMM) is used here to get the saddle point of (2). The mode number  $K$  is determined in advance. Then the frequency-domain expression of mode  $\{\widehat{u}_k^1\}$ , the corresponding center frequency  $\{\widehat{\omega}_k^1\}$ , and the Lagrangian multiplier  $\{\widehat{\lambda}^1\}$  are initialized. The modes  $u_k$  and their center frequency  $\omega_k$  are updated by (3) and (4) respectively.

$$\widehat{u}_k^{n+1}(\omega) = \frac{\widehat{f}(\omega) - \sum_{i \neq k} \widehat{u}_i(\omega) + \frac{\widehat{\lambda}(\omega)}{2}}{1 + 2\alpha(\omega - \omega_k)^2} \quad (3)$$

$$\omega_k^{n+1} = \frac{\int_0^\infty \omega |\widehat{u}_k(\omega)|^2 d\omega}{\int_0^\infty |\widehat{u}_k(\omega)|^2 d\omega} \quad (4)$$

After each updating of modes and center frequencies, the Lagrangian multiplier is also updated by (5).

$$\widehat{\lambda}^{n+1}(\omega) \leftarrow \widehat{\lambda}^n(\omega) + \tau \left[ \widehat{f}(\omega) - \sum_k \widehat{u}_k^{n+1}(\omega) \right] \quad (5)$$

The updating process is executed iteratively until (6) is satisfied.

$$\sum_k \left\| \widehat{u}_k^{n+1} - \widehat{u}_k^n \right\|_2^2 / \left\| \widehat{u}_k^n \right\|_2^2 < e \quad (6)$$

## 2.2. Kernel-Based Fuzzy c-Means Clustering

Pattern recognition is one of the most important tasks in mechanical fault diagnosis. The kernel-based fuzzy c-means clustering (KFCM) [39] is an effect classification algorithm, which can map low-dimensional data into high-dimensional space by kernel function to enlarge the difference between samples. Moreover, KFCM has no learning process for a large amount of data in the previous stage. The brief computational steps are as follows:

1. Select the cluster number  $c$  and input  $n$  dataset  $X = \{x_1, x_2, \dots, x_n\}$ ,  $X \subseteq R^p$  to be classified.
2. Perform an arbitrary non-linear mapping  $\Phi$  from the original low-dimensional feature space  $K$  to a space of higher kernel space  $F$ .
3. Assume that  $v_i (i = 1, 2, \dots, c)$  is the cluster centroid of  $i$ th cluster, and  $u_{ik} (k = 1, 2, \dots, n)$  is the membership degree of data point  $x_k$  to  $i$ th cluster. Then the objective function of KFCM algorithm is as below:

$$J_m(U, v) = \sum_{i=1}^c \sum_{k=1}^n u_{ik}^m \left\| \Phi(x_k) - \Phi(v_i) \right\|^2, \quad (7)$$

where  $U = \{u_{ik}\}$ ,  $v = \{v_1, v_2, \dots, v_c\}$ ,  $m > 1$ , which is the weight index to membership matrix  $U$ .

4. Chose the radial basis function as the kernel function without prior knowledge, whose expression is presented as (8):

$$K(x_k, v_i) = \exp[-\|x_k - v_i\|^2 / (2\sigma^2)], \quad (8)$$

where  $v_i$  is the center of the kernel function and  $\sigma$  is the width parameter. After introducing a kernel function, the (7) can be expressed as follow:

$$J_m(U, v) = \sum_{i=1}^c \sum_{k=1}^n u_{ik}^m \left\| 2 - 2K(x_k, v_i) \right\|^2. \quad (9)$$

5. Search the minimum valve of objective function (9) using the Lagrange multiplier optimization method. Finally, the iteration formulas of  $u_{ik}$  and  $v_i$  can be obtained:

$$u_{ik} = \frac{\{1/[K(x_k, x_k) + K(v_i, v_i) - 2K(x_k, v_i)]\}^{1/(m-1)}}{\sum_{j=1}^c \{1/[K(x_k, x_k) + K(v_j, v_j) - 2K(x_k, v_j)]\}^{1/(m-1)}}. \quad (10)$$

$$v_i = \sum_{k=1}^n u_{ik}^m K(x_k, v_i) x_k / \sum_{k=1}^n u_{ik}^m K(x_k, v_i). \quad (11)$$

### 2.3. A Parameter-Optimized Variational Mode Decomposition

During the research of conventional VMD algorithm, it was found that the mode number  $K$  has significant influence on the decomposition results. The mode number  $K$  should be given in advance in conventional VMD, which will inevitably lead to uncertainty of results. If  $K$  is too small, multiple components of the original signal may be contained in one mode function. If  $K$  is too large, one component may be decomposed into several mode functions. All of the above will lead to errors in estimating IMF center frequency. Scholars have done a lot of research on the optimal selection of  $K$  value. Some scholars choose the  $K$  value by experience e.g., [43–45], which are inefficient and not applicable to large amount of data processing. Yan X et al. [34] used genetic algorithm to optimize the mode number  $K$  in VMD and combined it with 1.5-dimensional envelope spectrum for fault diagnosis of rotating machinery. However, the optimization method proposed in [22–24,46] will increase the complexity of VMD algorithm and reduce the efficiency of fault diagnosis. Correlation coefficient was introduced due to its effectiveness for measure the correlation degree of IMF and original signal and distinguish the effective components from noise components [25–27]. It is found that the decomposition results tend to be stable when  $K$  reaches a certain value in VMD. Therefore, a novel  $K$  selection method based on the correlation coefficient analysis was proposed in this article. The detailed procedure is as below:

1. Determine the range of  $K$  that needs to be optimized.
2. Decompose the original signal by VMD in the selected  $K$  range. For each  $K$  value, two parameters are calculated, including the correlation coefficient between IMFs and the original signal and the energy ratio of the residual to the original signal.
3. Any IMF with a correlation coefficient greater than the threshold  $C$  is called an effective IMF (EIMF), and the number of EIMF is counted at each  $K$ . When the count of EIMF number keeps steady in the range of  $K$ , the result of signal decomposition is considered stable.
4. After stable decomposition, when the energy ratio of the residual is less than 0.3 for the first time, the corresponding  $K$  value is regarded as the optimal  $K$  value. Then, output the EIMFs at the optimal  $K$ .

The correlation coefficient between the IMF and the original signal can be used to judge whether the IMF is a false mode caused by noise. The correlation coefficient is calculated as follows:

$$r(x, y) = \frac{Cov(x, y)}{\sqrt{Var[x] \cdot Var[y]}}, \quad (12)$$

where  $x$  and  $y$  represent two different signals,  $Cov$  is the covariance symbol and  $Var$  is the variance symbol. The calculation formula of the energy ratio  $R$  is as follows:

$$R = \frac{E_o - E_r}{E_o} = \frac{\int_{-\infty}^{+\infty} f^2(t) dt - \int_{-\infty}^{+\infty} \left[ \sum_{k=1}^n u_k(t) \right]^2 dt}{\int_{-\infty}^{+\infty} f^2(t) dt}, \quad (13)$$

where  $E_o$  and  $E_r$  represent the original signal energy and the reconstructed signal energy respectively.  $f(t)$  is the original signal.  $u_k(t)$  are the IMFs of VMD.

$R$  is the energy ratio of the residual to the original signal. Since the noise energy is large for the actual diesel engine signal, when the energy of the reconstructed signal reaches more than 0.7 of the original signal, the decomposition is basically complete. This empirical value can be modified according to the actual signal noise.

The quadratic penalty factor  $\alpha$  affects the de-noise ability of VMD algorithm. Many scholars optimized it with  $K$  together [22–24]. A similar analysis has been done for the vibration signal of diesel engine, it is found that the decomposition effect is comparatively more sensitive to the  $k$  value by analyzing the decomposition results under a series of different  $K$  and  $\alpha$ . Therefore, the default value of  $\alpha$ , 2000, was used in this article.

To verify the effectiveness of the proposed method, the algorithm was used to decompose a set of simulation signals. The reciprocating nature of diesel engine results in the periodic vibration signals of cylinder head. In addition, the movement of the piston and the valve of the diesel engine will cause different degrees of cylinder head impulse signals. Therefore, simulation signal  $y(t)$  consists of three periodic sinusoidal signals  $x_1(t)$ ,  $x_2(t)$ , and  $x_3(t)$ , which have different frequencies and a set of composite impulse signals  $x_4(t)$ . In order to simulate the real vibration signal of diesel engine, the random signal with amplitude ranging from  $-20$  to  $20$  was added. The expressions of the constituent signals are shown in (14) and the simulation signal is shown in Figure 1.

$$\left\{ \begin{array}{l} x_1(t) = 60 * \sin(100\pi t) \\ x_2(t) = 40 * \sin(800\pi t) \\ x_3(t) = 40 * \sin(3500\pi t) \\ x_4(t) = \begin{cases} 100 * \sin(1200\pi t), 0.0045 < t < 0.011 \\ 50 * \sin(1000\pi t), 0.025 < t < 0.035 \\ 0, other \end{cases} \\ y(t) = x_1(t) + x_2(t) + x_3(t) + x_4(t) \end{array} \right. \quad (14)$$

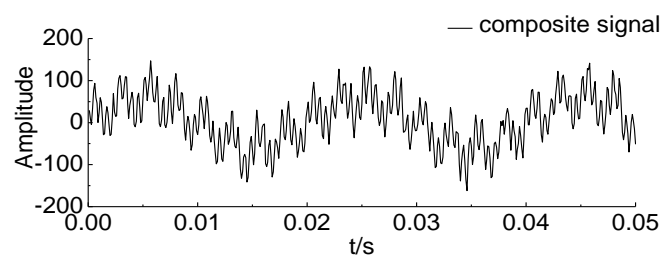
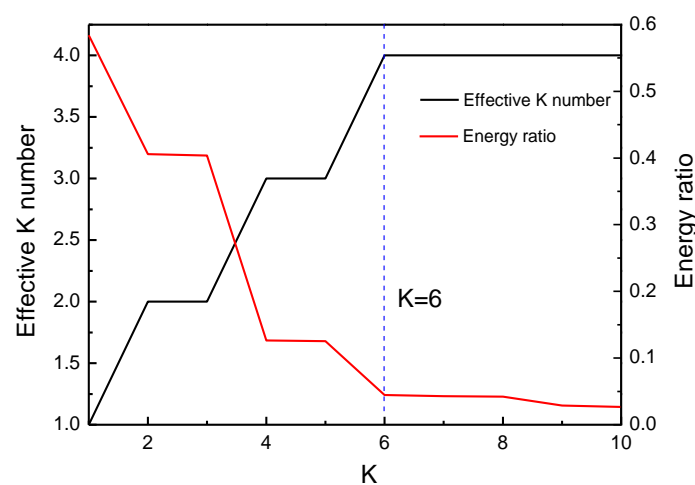


Figure 1. Simulation signal.

Next, the simulation signal was decomposed simultaneously via the optimized-VMD, EMD, LMD and EEMD algorithm. For the proposed algorithm, the range of  $K$  value was set to 1–10, and the correlation coefficient threshold  $C$  was 0.35. Some correlation coefficient results between the IMFs and the original signal at each  $K$  is shown in Table 1. The curves of effective  $K$  value and energy ratio is shown in Figure 2. It can be inferred from the Figure 2 that the decomposition results were stable when the mode number was over 6, where EIMF number remained at 4. At the same time, the energy ratio was also below 0.3, so the optimal  $K$  value was 6.

**Table 1.** The correlation coefficient between intrinsic mode functions (IMFs) and the original signal.

C	K = 3	K = 4	K = 5	K = 6	K = 7	K = 8	K = 9
IMF1.	0.76	0.65	0.65	0.63	0.63	0.63	0.63
IMF2	0.45	0.63	0.63	0.52	0.52	0.52	0.48
IMF3	0.12	0.43	0.43	0.43	0.43	0.43	0.37
IMF4	-	0.07	0.07	0.44	0.44	0.43	0.42
IMF5	-	-	0.06	0.06	0.11	0.11	0.34
IMF6	-	-	-	0.05	0.06	0.05	0.10
IMF7	-	-	-	-	0.05	0.05	0.05
IMF8	-	-	-	-	-	0.04	0.05
IMF9	-	-	-	-	-	-	0.04
EIMF Number	2	3	3	4	4	4	4

**Figure 2.** Curves of two main parameters.

The VMD decomposition results at  $K = 6$  are shown in Figure 3. It can be seen from the figure that these four components are well restored and the false noise components are filtered out at the same time. Figure 4 shows the EMD decomposition results of  $y(t)$ , in which the simulation signal is decomposed into five IMFs and a residue. Figure 5 shows the decomposition results of  $y(t)$  by LMD, where the simulation signal was decomposed into three product functions (PF). In comparison, the results of EMD and LMD appeared that an obvious mode aliasing phenomenon and signal distortion led to incomplete sinusoidal waveform. This is due to the accumulation of error in envelope estimation. The decomposition results of EEMD are shown in Figure 6. As an improved version of EMD, EEMD effectively suppressed the mode aliasing problem of EMD. It had better decomposition effect for shock signal  $x_4(t)$ . However, there still existed the mode aliasing problem in IMF2–IMF4. In addition, the increase of white noise led to the low computational efficiency of EEMD. The variational structure of VMD had better robustness to noise and improved the mode aliasing of the recursive decomposition algorithms. Moreover, it can be seen that the end effect of EMD/LMD was more serious than that of VMD.

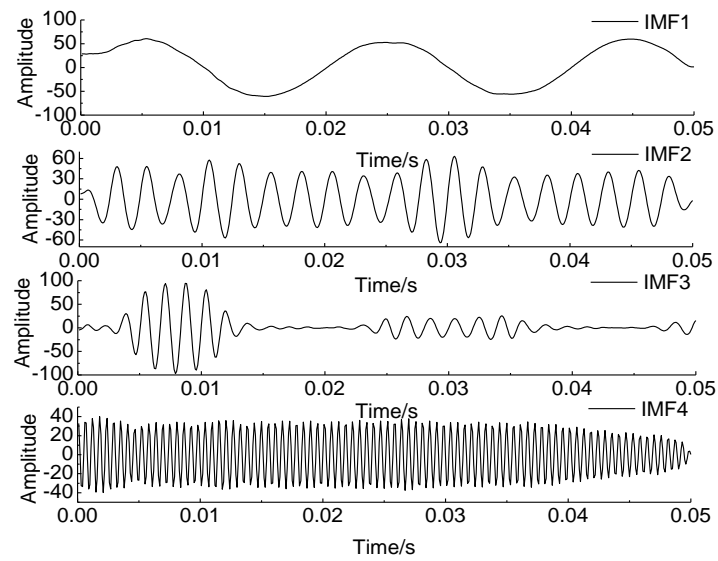


Figure 3. Optimized-variational mode decomposition (VMD) results of simulation signal  $y(t)$ .

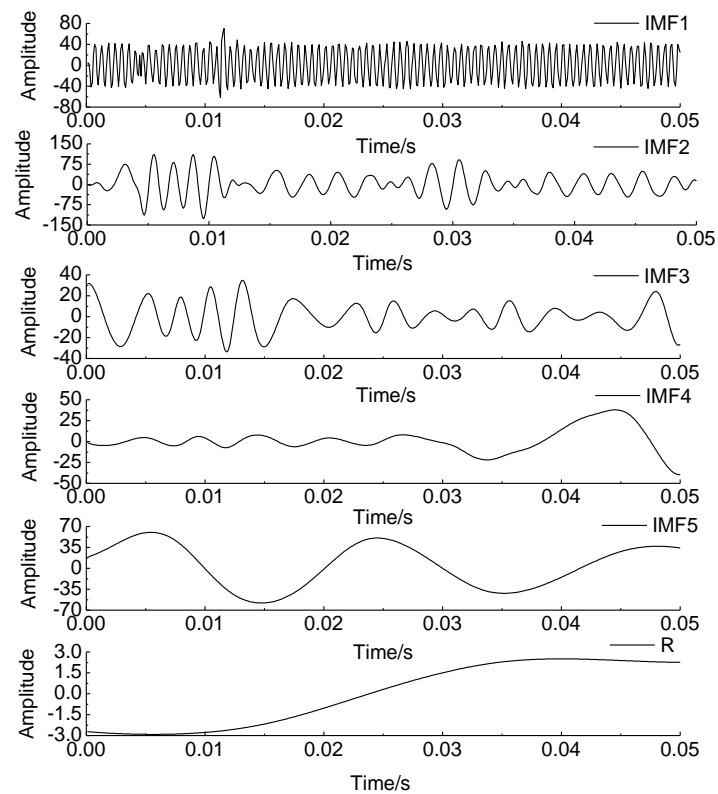


Figure 4. Empirical mode decomposition (EMD) results of simulation signal  $y(t)$ .

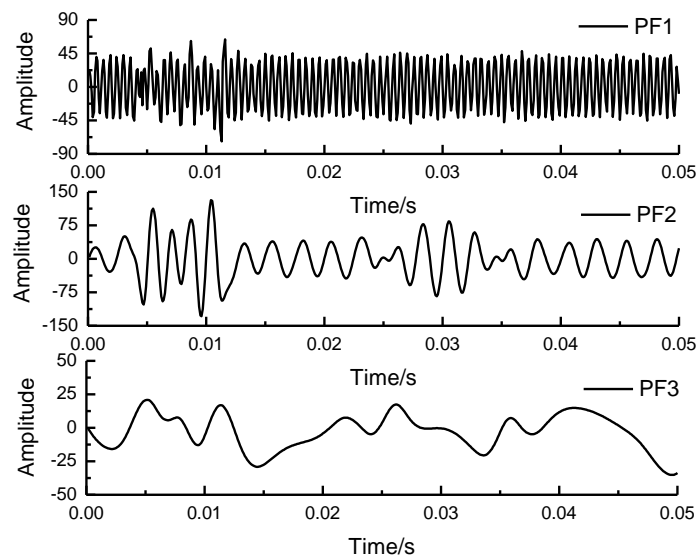


Figure 5. Local mean decomposition (LMD) results of simulation signal  $y(t)$ .

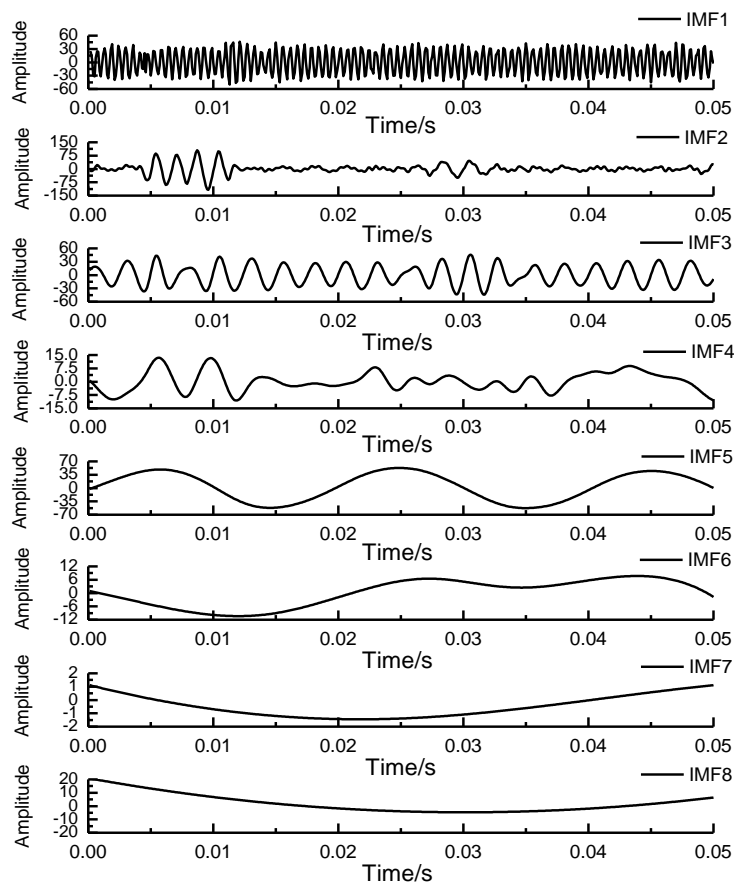


Figure 6. EEMD results of simulation signal  $y(t)$ .

To further verify the superiority of VMD decomposition algorithm, the correlation coefficients were calculated between decomposition results of each algorithm and four components of original signal. Then the maximum correlation coefficients with each component of original signal were recorded. The results are shown in Table 2. It can be seen that the correlations between the result components of EMD/LMD and the original signal components was significantly lower than that of EEMD/VMD. The correlation of optimized-VMD was the highest among these four algorithms.

VMD had a good decomposition effect not only for single frequency sinusoidal components, but also for mixed impulse signals, which were difficult to decompose.

**Table 2.** Statistical table of maximum correlation coefficient.

Maximum Correlation Coefficient	EMD	LMD	EEMD	VMD
$x_1(t)$	0.459	0.437	0.994	0.996
$x_2(t)$	0.113	0.708	0.909	0.937
$x_3(t)$	0.004	0.950	0.957	0.991
$x_4(t)$	0.055	0.694	0.880	0.915

As mentioned above, there are two parameters, the range of  $K$  and correlation coefficient threshold  $C$ , that need to be set in advance in the proposed method. The range of  $K$  values needs to be large enough to make the decomposition result stable. Experiments show that when the mode number was more than twice the signal component number, it was easy to cause over-decomposition. Excessive  $K$  value will increase unnecessary calculation cost. Over-decomposition will reduce the accuracy of pattern recognition. For signals with less components ( $\leq 6$ ), the range of  $K$  can be empirically set from 1 to 10 or twice the number of components. The empirical  $K$ -value range could ensure that most decomposition results are stable. For the cylinder head vibration signal in this paper, the main components of the signal include the combustion impulse, opening and closing impulse of the intake and exhaust valve, reciprocating impact of piston, and so on. However, due to the periodicity of diesel engine vibration signals, the number of components is usually no more than 6. Therefore, this range is also suitable for the cylinder head vibration signal.

To validate the threshold of correlation coefficient, 40 sets of simulation signals with known components were decomposed by optimized-VMD in which  $C$  was varied from 0.25 to 0.4. According to the comparison of maximum correlation coefficients between the IMFs of the decomposition results and the components of the original signal, the correct rate of decomposition is shown in Figure 7. It can be seen that the correct rate of different  $C$  within the range was significantly different, but there was an obvious peak, where the decomposition accuracy reached the maximum 97.5% when  $C = 0.35$ . Therefore, the value of  $C$  was set to 0.35 in this paper.

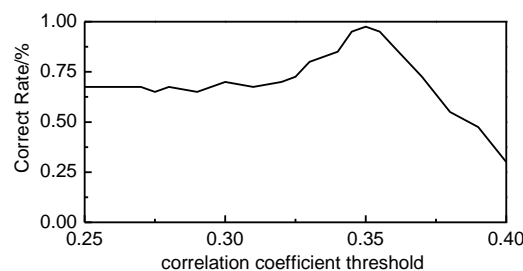


**Figure 7.** The accuracy of decomposition.

### 3. Fault Simulation Bench Test

To verify the effectiveness of the proposed algorithm for real vibration signals decomposition, the real cylinder head vibration signals of a certain diesel engine were analyzed in this section. The six-cylinder diesel engine is an in-line, water-cooled four-stroke engine with four valves per cylinder. Figure 8a shows the diesel engine tested on the bench, and the technical parameters of the diesel engine are listed in Table 3. Vibration acceleration sensors (PCB-621B40, PCB Piezotronics Inc., New York, NY, USA) were fixed on the cylinder head of 1-6th cylinder and cylinder block of 1-6th cylinder as the Figure 8b shown. Vibration signals were collected by the LMS-SCADAS Mobile multi-channel high-speed data acquisition system.

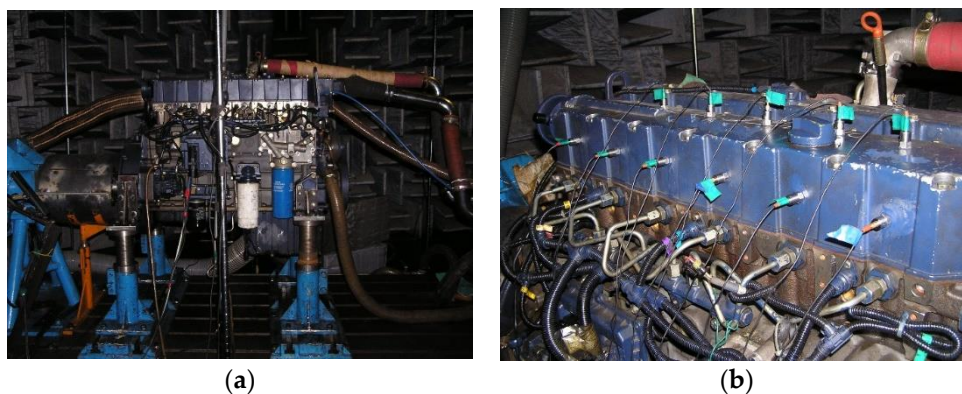


**Figure 8.** Fault simulation test diesel engine: (a) test diesel engine on bench and (b) position of vibration acceleration sensors.

**Table 3.** Main parameters of a certain type of diesel engine.

Contents	Parameters
Number of cylinder	Inline 6 cylinders
Valve number/cylinder	4
Displacement	7.14 L
Cylinder diameter/length	108 mm/130 mm
Power rating/rated speed	220 kW/2300 r/min
Maximum torque	11,600 Nm (1200–1600 r/min)

The frequency of diesel engine vibration signal generally distributes in the range of 0–6000 Hz. When rough combustion occurs, high frequency vibration will propagate, but still not more than 12,000 Hz. So, the analysis frequency was set to 12,800 Hz in the test, the sampling frequency was 25 and 600 Hz. The test stimulated three typical types of faults including abnormal valve clearance, abnormal common rail pressure, and insufficient fuel supply, where details are described in Table 4. The steady vibration signal of diesel engine was measured with speed increment of 100 rpm beginning from 800 rpm (idle speed) to 2300 rpm (rated speed). We chose the vibration signal when the speed of diesel engine was stable at 2000 rpm.

**Table 4.** Simulated faults details.

Abnormal Valve Clearance/mm	Abnormal Common Rail Pressure/bar	Insufficient Fuel Supply
Reduce (0.25, 0.45)	Normal 1500	Normal 100%
Normal (0.30, 0.50)	Reduce 1300	Reduce 75%
Increase (0.35, 0.55)	Reduce 1100	Reduce 25%
Increase (0.40, 0.60)	-	-

Where '(0.25, 0.45)' means that the inlet valve clearance is 0.25 mm, the exhaust valve clearance is 0.45 mm, and so does the rest.

#### 4. Fault Diagnosis Based on Optimized-VMD and KFCM

As mentioned above, the signal components can be obtained ideally by decomposition of the optimized-VMD algorithm. However, only using VMD is not clear enough to reveal the occurrence of the faults. In order to identify the faults effectively and improve the diagnosis speed, we combined VMD and KFCM to unite the advantages of these two algorithms. KFCM is a pattern recognition algorithm without supervised learning. Three-dimensional KFCM has a better visualization effect and higher classification accuracy than the two-dimensional ones. The concrete steps for joint diagnosis are as follows:

1. The optimized-VMD algorithm was used to decompose the cylinder head signal adaptively and output the IMFs.
2. The parameters of three IMFs with relative maximal correlation coefficient to the original signal were extracted. The appropriate parameters were selected to form a three-dimensional feature vector group.
3. The three-dimensional feature vectors were input into the KFCM for classification and obtained the results.

To verify the effectiveness of fault diagnosis method, the optimized-VMD was used to decompose the valve clearance fault signals including three different states here according to Table 4, including reduction (0.25, 0.45), increase (0.35, 0.55), and increase (0.40, 0.60). The optimum range of  $K$  value of mode number was set to 1–10. The threshold of correlation coefficient was set to 0.35. Figure 9 shows the curves of EIMF number and energy ratio  $R$  of valve clearance reduction (0.25, 0.45). It can be inferred that when  $K$  was greater than 3, the decomposition was stable and the energy ratio  $R$  was also below 0.3. Therefore, the optimized  $K$  value was 3. Figures 10–12 show the VMD decomposition results of the above three signals respectively, where the left column represents IMFs and the right column are the corresponding power spectral density (PSD) in the frequency domain. It can be seen from these figures that the main vibration frequency was about 2000 Hz when a valve clearance fault occurred. When the valve clearance was increased to (0.4, 0.6) state, a peak appeared at the frequency of 2500 Hz. However, it was difficult to distinguish between reduced valve clearance (0.25, 0.45) and increased valve clearance (0.35, 0.55). It is important to choose appropriate parameters to describe the characteristics of signals and to amplify the differences.

We compared the classification results of ten more parameters such as mean value, standard deviation, kurtosis, permutation entropy, and so on. However, the classification effect of most parameters was not good. Here we selected four representative parameters to show the classification results, including root mean square value (RMS), kurtosis (Kur), Shannon entropy (SE), and singular value (SV). Seventy-five sets of experimental signals were intercepted from each fault state data for testing. Each signal was intercepted for 0.06 seconds, which is the time of about a cycle for the diesel engine at the speed of 2000 rpm.

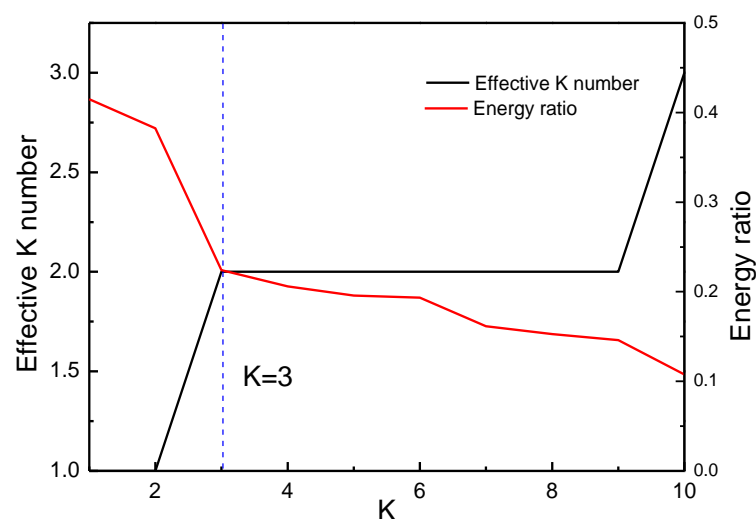


Figure 9. Curves of two main parameters of valve clearance reduction (0.25, 0.45).

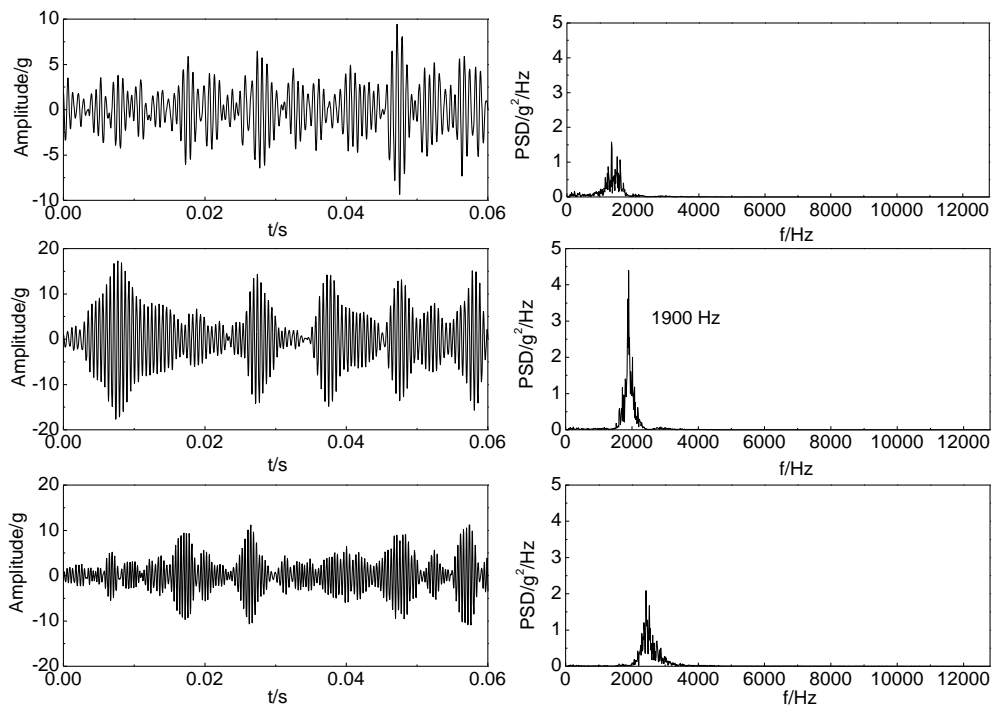


Figure 10. The VMD result of valve reduction (0.25, 0.45).

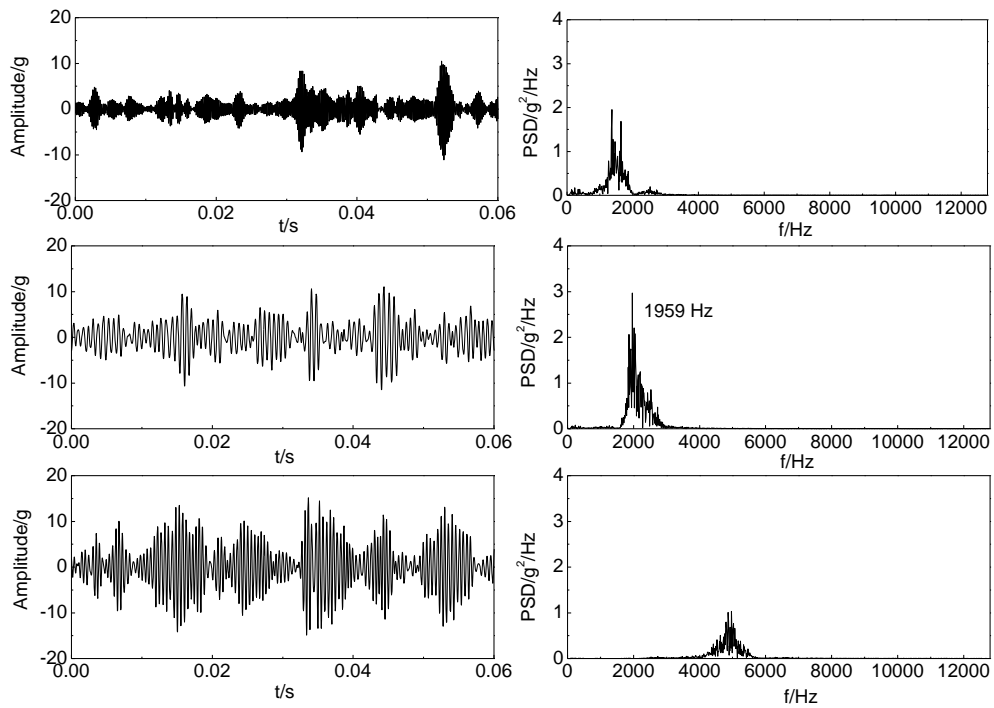
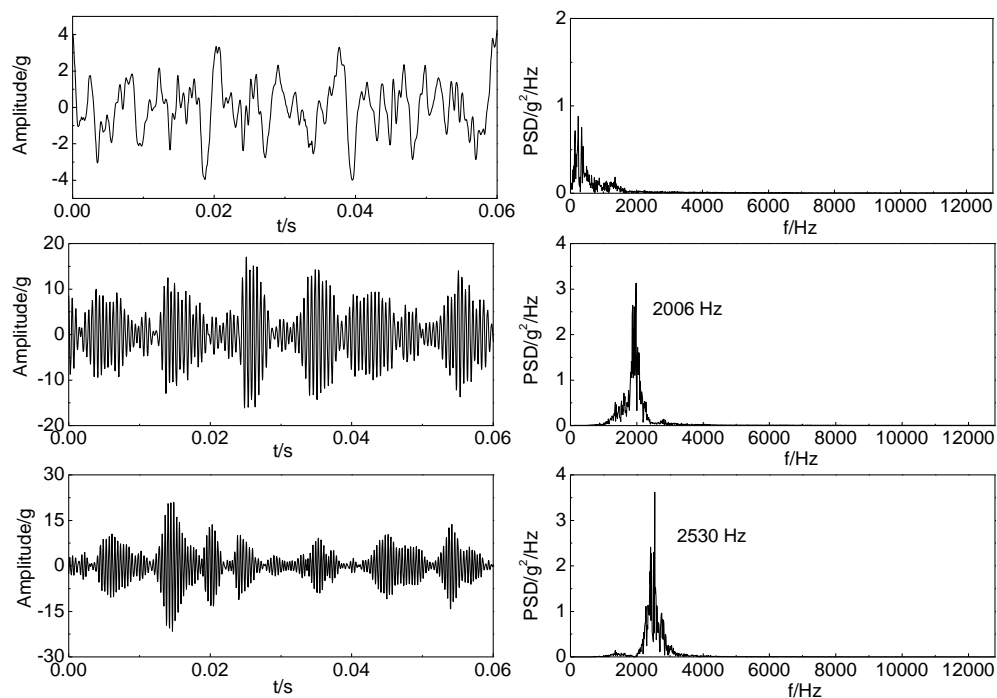


Figure 11. The VMD result of valve increase (0.35, 0.55).



**Figure 12.** The VMD result of valve increase (0.40, 0.60).

The three-dimensional feature vectors are input into KFCM for classification. The fuzzy weighted index  $m$  of KFCM was set to 1.5, and the square of radial basis function width  $\sigma^2$  was set to 250. The classification results of KFCM algorithm are shown in Figure 13a–c. Figure 13a shows that the classification effect of RMS was not satisfactory. Three valve clearance reduction states could not be well distinguished. Many points of increase (0.35, 0.55) and increase (0.40, 0.60) were misclassified into the reduction (0.25, 0.45). The total classification accuracy was 86.2%. From Figure 13b, it can be seen that Shannon entropy as the feature vector had a worse classification effect than RMS. Since the difference between the two types of fault data was small, the reduction (0.25, 0.45) points and the increase (0.40, 0.60) points were misclassified into one class. When kurtosis was used as the feature vector for classification, three kinds of faults were clustered together and could not be distinguished at all, so the results are not shown here. Figure 13c shows the KFCM classification result when singular values were used as feature vectors. From Figure 13c, we could see that the data of three different states were well distinguished, and the boundaries were obvious. Compared with the previous parameters, the classification effect was greatly improved, and the correct rate was significantly improved. Only four of 225 data points were misclassified, and the correct rate had reached 98.2%. For comparison, Figure 13d shows the classification results of abnormal valve clearance fault signals and normal signals. The VMD-KFCM joint algorithm could still distinguish four kinds of data points very well. Based on the above results, the singular values were used as feature vectors in the next fault diagnosis.

In order to further verify the effectiveness of VMD-KFCM algorithm, the common rail pressure abnormal fault data and insufficient fuel supply fault data were then diagnosed. Fifty sets of data were used to diagnose each fault. The range of  $K$  values was set to 1–10, and the threshold of correlation coefficient was set to 0.35. Singular values were still selected as the feature parameters here. The parameters of KFCM were set as above. Figure 14a,b show the diagnostic results of insufficient fuel supply signals and abnormal common rail pressure signals, respectively. For the final fault diagnosis accuracy, the two kinds of faults were 98.7% and 96%. Obviously, the proposed VMD-KFCM algorithm could obtain good decomposition results for three different fault state signals of the diesel engine. It has a high diagnostic accuracy rate for different degrees signals of a certain fault.

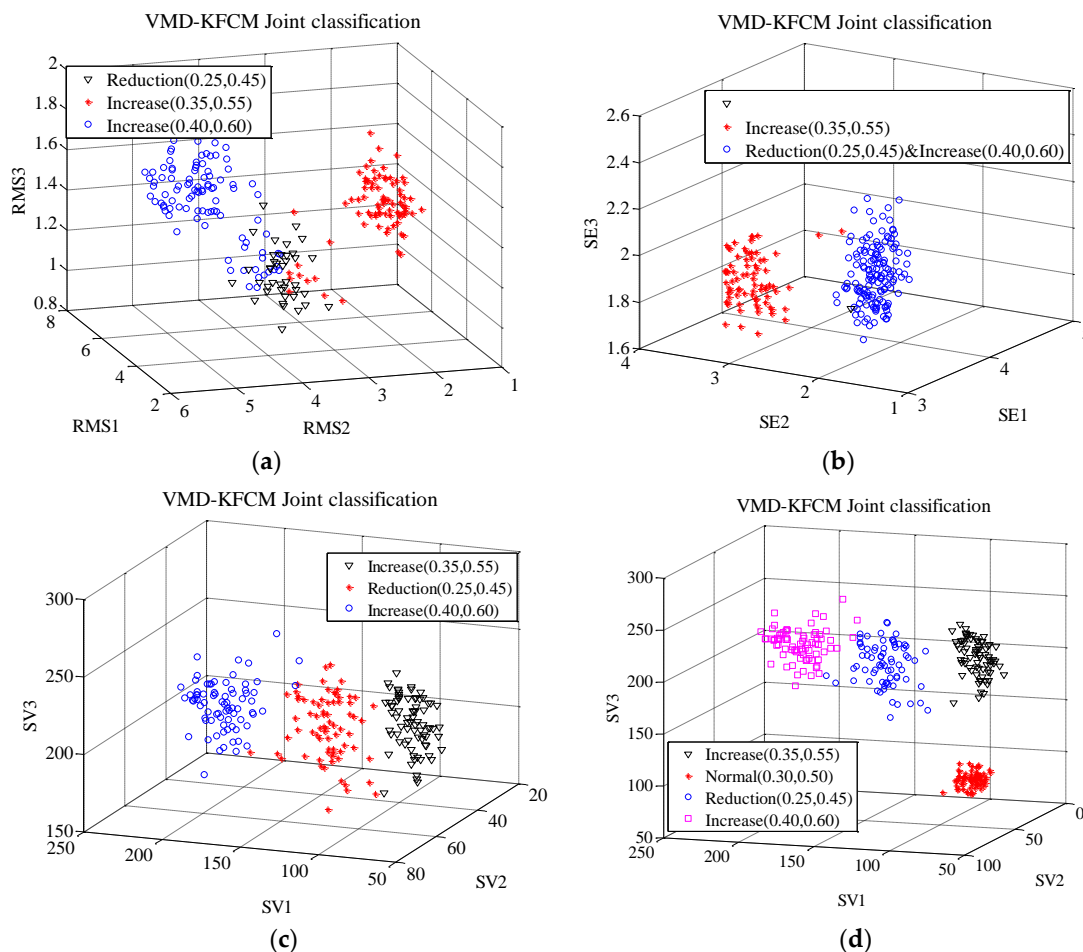


**Figure 13.** VMD-kernel-based fuzzy c-means clustering (KFCM) classification result of abnormal valve clearance signals: (a) root mean square value (RMS) as feature vector; (b) Shannon entropy as feature vector; (c) singular value as feature vector; and (d) distinction between normal signals and abnormal valve clearance signals using singular value as feature vector.

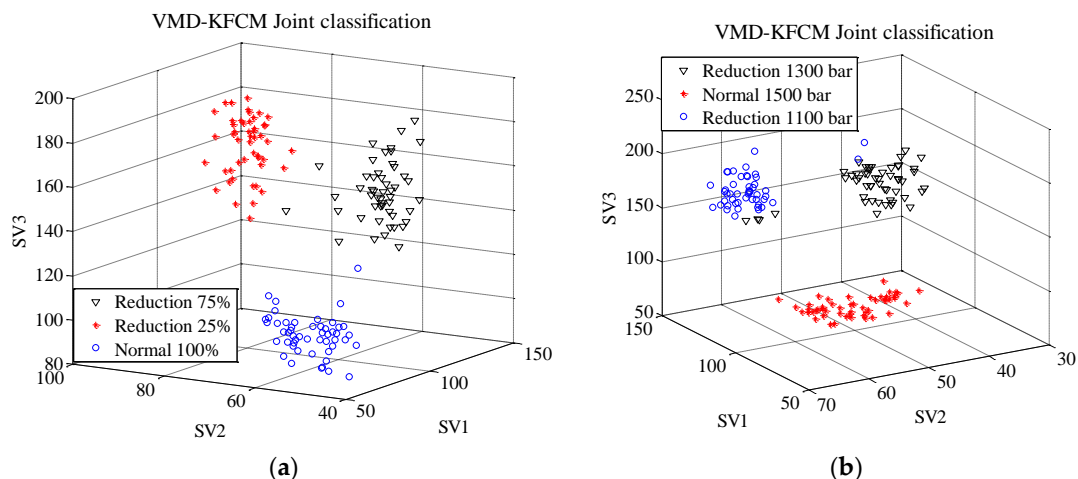


**Figure 14.** VMD-KFCM classification results: (a) classification result of insufficient fuel supply signals and (b) classification result of abnormal common rail pressure signals.

For comparison, EMD/EEMD and KFCM were combined to diagnose the same signals above. EMD/EEMD was used to adaptively decompose the original signal into multiple IMFs. The parameter setting of KFCM algorithm was the same as above. Three IMFs with the highest correlation to original

signal were used to compute feature vectors to input KFCM algorithm. Here, we still chose singular values as feature vectors. Figure 15a–c shows the classification results of the EMD-KFCM method for abnormal valve clearance, insufficient fuel supply, and abnormal common rail pressure, respectively. Obviously, the classification effect of EMD-KFCM was not as good as VMD-KFCM. The boundaries between different types of data points were not clear enough, and data points of the same fault were not centralized. The accuracy of EMD-KFCM fault classification was much lower than that of the proposed method. In addition, the result of EEMD-KFCM fault diagnosis was better than EMD-KFCM. Especially for insufficient fuel supply, the accuracy of diagnosis increased obviously. However, the overall accuracy was still lower than the proposed algorithm. The comparison of the accuracy of three algorithms is shown in Table 5.

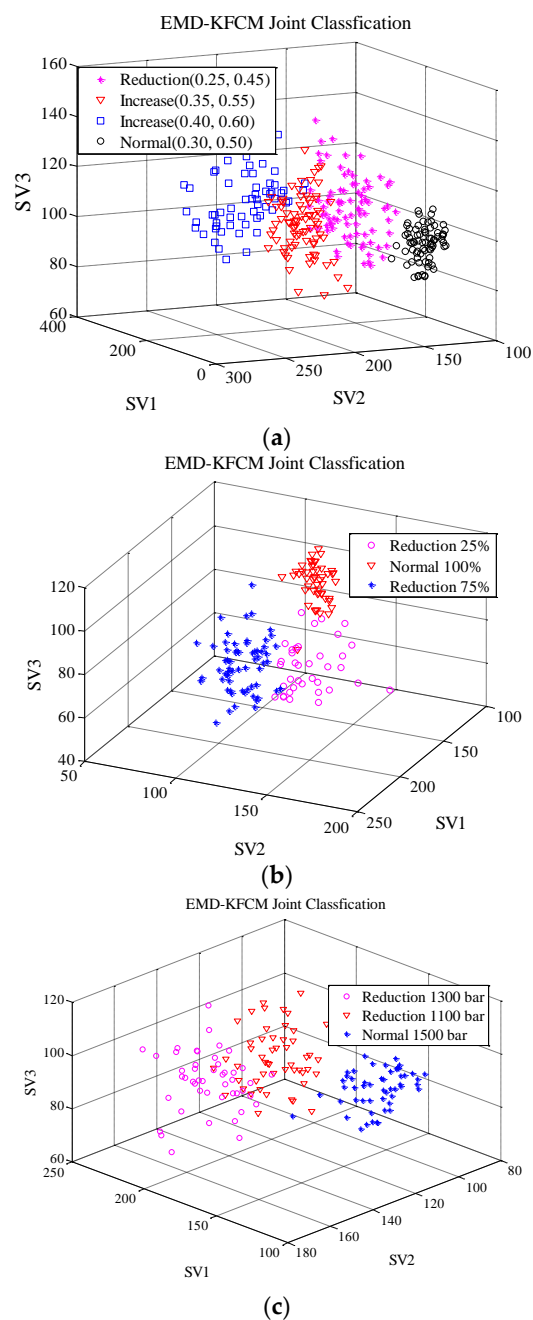


**Figure 15.** EMD-KFCM classification results: (a) classification result of abnormal valve clearance; (b) classification result of insufficient fuel supply signals; and (c) classification result of abnormal common rail pressure signals.

Next, supervised learning methods, BPNN and DBN, were used to classify the same faults for comparison. BPNN was combined with the optimized-VMD, which means that the BPNN were trained and tested by the three-dimensional feature vectors of VMD. In this paper, layer of BPNN was set as 3 and the number of neurons in the hidden layer was 10 [34]. Here, another 50 sets of data in different condition respectively were selected for training. After that, the same input data as VMD-KFCM example were classified by trained BPNN and classification accuracy is shown in Table 5. The classification accuracy of abnormal common rail pressure fault was only 74.7%, but the accuracy of the other two kinds of fault was high. DBN has an excellent feature abstraction and data mining ability, so 100 sets of original data in different condition respectively were used to train DBN directly. There are two restricted Boltzmann machine (RBM) layers in DBN, and the number of neurons in each hidden layer is 100. The momentum of each RBM was set to 0.5 [36]. The size of “mini-batches” was set to 10 [47]. The learning rate was set to 1. However, DBN cannot effectively separate the faults without VMD. This may be due to the complexity of engine vibration signals, or the insufficient samples. Therefore, three-dimensional maximum singular values of IMFs were used to train and test DBN. As shown in Table 5, the results were still not ideal. Next, more feature vectors were selected to train DBN. For the three IMFs with relative maximal correlation to original signal, we calculated seven kinds of parameters: the maximum singular value, kurtosis, Shannon entropy, root mean square value, energy, fourth-order cumulant, and multi-scale sample entropy. At last, 21 dimensional feature vectors were used to train DBN, and the final classification accuracy is shown in Table 5. For abnormal valve clearance data, VMD-DBN was better than VMD-KFCM, and the classification accuracy was 100%. However, for the other two types of faults, VMD-KFCM still had a higher accuracy. The results show that the deep learning method may need higher dimensions and more data for complex training to get better results. Obviously, the proposed method had advantages in calculation efficiency and algorithm simplicity.

**Table 5.** Comparison of classification accuracy.

Fault Classification Accuracy	Abnormal Valve Clearance	Abnormal Common Rail Pressure	Insufficient Fuel Supply
VMD-KFCM	98.2%	96%	98.7%
EMD-KFCM	68.8%	82%	83.3%
EEMD-KFCM	68.4%	82%	98%
VMD-BPNN	90%	74.7%	94%
DBN	/	/	/
VMD-DBN (3D)	66.7%	34.7	65.3%
VMD-DBN (21D)	100%	81.3%	94.7%

## 5. Conclusions

To achieve accurate, efficient, and adaptive identification of diesel engine faults, a novel fault diagnosis method based on optimized-VMD and KFCM was proposed in this paper. Firstly, the correlation coefficient and energy ratio were used to optimize the mode number  $K$ , so that the VMD algorithm could adaptively select the best  $K$  value for decomposition. Through the verification of simulation signals, the decomposition effect of optimized-VMD was better than EMD, LMD, and EEMD. Then VMD was combined with the KFCM algorithm. After comparing various parameters, maximum singular values were input into KFCM as feature vectors for classification. Then three different kinds of diesel engine faults were simulated in a bench test, and the vibration signals of the machine surface were collected. To prove the effectiveness of VMD-KFCM, the proposed method was compared with EMD-KFCM, EEMD-KFCM, VMD-BPNN, and VMD-DBN. The experimental results show that the proposed method had obvious advantages in classification accuracy, simplicity, and efficiency. Finally, the diagnosis accuracy of abnormal valve clearance, abnormal common rail pressure and insufficient fuel supply were 98.2%, 96%, and 98.7%, respectively.

However, there were still some further works to finish. Other parameters in VMD, such as quadratic penalty, and the structure of the algorithm could be optimized to improve the effectiveness of decomposition. Besides, the comparisons with supervised learning methods in this paper was insufficient, the advantages of BPNN and DBN might not be fully exploited.

**Author Contributions:** Conceptualization, X.B., J.L., D.T. and F.B.; data curation, T.M.; formal analysis, X.L. and T.M.; funding acquisition, F.B.; investigation, X.Y.; resources, P.S.; supervision, J.L. and F.B.; validation, X.L., X.Y. and P.S.; writing—original draft, X.B.; writing—review and editing, D.T. All authors have read and agreed to the published version of the manuscript.

**Funding:** This research was supported by “National Natural Science Foundation of China: Project 51705357.” and “National Science and Technology Support Program of China: Vibration and Noise Reduction Technology Research and Application of Bulldozers and Other Earth Moving Machinery (Grant No. 2015BAF07B04)”.

**Acknowledgments:** This research received no other support, which is not covered by author contribution or funding sections.

**Conflicts of Interest:** The authors declare no conflict of interest.

## References

1. Kimmich, F.; Schwarte, A.; Isermann, R. Fault detection for modern Diesel engines using signal- and process model-based methods. *Control Eng. Pract.* **2005**, *13*, 189–203. [[CrossRef](#)]
2. Lei, Y.; Lin, J.; He, Z.; Zuo, M.J.; Zuo, M. A review on empirical mode decomposition in fault diagnosis of rotating machinery. *Mech. Syst. Signal Process.* **2013**, *35*, 108–126. [[CrossRef](#)]
3. Rai, A.; Upadhyay, S. A review on signal processing techniques utilized in the fault diagnosis of rolling element bearings. *Tribol. Int.* **2016**, *96*, 289–306. [[CrossRef](#)]
4. Flett, J.; Bone, G.M. Fault detection and diagnosis of diesel engine valve trains. *Mech. Syst. Signal Process.* **2016**, *72*, 316–327. [[CrossRef](#)]
5. Jiang, Z.; Mao, Z.; Wang, Z.; Zhang, J. Fault Diagnosis of Internal Combustion Engine Valve Clearance Using the Impact Commencement Detection Method. *Sensors* **2017**, *17*, 2916. [[CrossRef](#)] [[PubMed](#)]
6. Huang, N.E.; Shen, Z.; Long, S.R.; Wu, M.C.; Shih, H.H.; Zheng, Q.; Yen, N.C.; Tung, C.C.; Liu, H.H. The empirical mode decomposition and the Hilbert spectrum for nonlinear and non-stationary time series analysis. *Proc. Math. Phys. Eng. Sci.* **1998**, *454*, 903–995. [[CrossRef](#)]
7. Smith, J.S. The local mean decomposition and its application to EEG perception data. *J. R. Soc. Interface* **2005**, *2*, 443–454. [[CrossRef](#)] [[PubMed](#)]
8. Liu, H.; Han, M. A fault diagnosis method based on local mean decomposition and multi-scale entropy for roller bearings. *Mech. Mach. Theory* **2014**, *75*, 67–78. [[CrossRef](#)]
9. Torres, M.E.; Colominas, M.A.; Schlotthauer, G.; Flandrin, P. A complete ensemble empirical mode decomposition with adaptive noise Eel. In Proceedings of the 2011 IEEE International Conference on Acoustics, Speech and Signal Processing (ICASSP), Prague, Czech Republic, 22–27 May 2011; pp. 4144–4147.
10. Li, Y.; Tse, P.W.T.; Yang, X.; Yang, J. EMD-based fault diagnosis for abnormal clearance between contacting components in a diesel engine. *Mech. Syst. Signal Process.* **2010**, *24*, 193–210. [[CrossRef](#)]
11. Qiao, N.; Wang, L.H.; Liu, Q.Y.; Zhai, H.Q. Multi-scale eigenvalues Empirical Mode Decomposition for geomagnetic signal filtering. *Measurement* **2019**, *146*, 885–891. [[CrossRef](#)]
12. Cheng, J.; Yu, D.; Yang, Y. Application of support vector regression machines to the processing of end effects of Hilbert–Huang transform. *Mech. Syst. Signal Process.* **2007**, *21*, 1197–1211. [[CrossRef](#)]
13. Wu, F.; Qu, L. An improved method for restraining the end effect in empirical mode decomposition and its applications to the fault diagnosis of large rotating machinery. *J. Sound Vib.* **2008**, *314*, 586–602. [[CrossRef](#)]
14. Wu, Z.; Huang, N.E. A study of the characteristics of white noise using the empirical mode decomposition method. *Proc. R. Soc. A Math. Phys. Eng. Sci.* **2004**, *460*, 1597–1611. [[CrossRef](#)]
15. Fengrong, B.; Teng, M.; Xu, W. Development of a novel knock characteristic detection method for gasoline engines based on wavelet-denoising and EMD decomposition. *Mech. Syst. Signal Process.* **2019**, *117*, 517–536.
16. Dragomiretskiy, K.; Zosso, D. Variational Mode Decomposition. *IEEE Trans. Signal Process.* **2014**, *62*, 531–544. [[CrossRef](#)]

17. Tang, G.; Wang, X.; He, Y.; Liu, S. Rolling bearing fault diagnosis based on variational mode decomposition and permutation entropy. In Proceedings of the International Conference on Ubiquitous Robots & Ambient Intelligence, Xi'an, China, 13 May 2016; pp. 626–631.
18. Liu, C.; Wu, Y.; Zhen, C. Rolling Bearing Fault Diagnosis Based on Variational Mode Decomposition and Fuzzy C Means Clustering. *Proc. CSEE* **2015**, *35*, 3358–3365.
19. Zhang, M.; Jiang, Z.; Feng, K. Research on variational mode decomposition in rolling bearings fault diagnosis of the multistage centrifugal pump. *Mech. Syst. Signal Process.* **2017**, *93*, 460–493. [[CrossRef](#)]
20. Liu, Y.; Yang, G.; Li, M.; Yin, H. Variational mode decomposition denoising combined the detrended fluctuation analysis. *Signal Process.* **2016**, *125*, 349–364. [[CrossRef](#)]
21. Yi, C.; Lv, Y.; Dang, Z. A Fault Diagnosis Scheme for Rolling Bearing Based on Particle Swarm Optimization in Variational Mode Decomposition. *Shock Vib.* **2016**, *2016*, 9372691. [[CrossRef](#)]
22. Zhang, X.; Miao, Q.; Zhang, H.; Wang, L. A parameter-adaptive VMD method based on grasshopper optimization algorithm to analyze vibration signals from rotating machinery. *Mech. Syst. Signal Process.* **2018**, *108*, 58–72. [[CrossRef](#)]
23. Wang, Z.; He, G.; Du, W.; Zhou, J.; Han, X.; Wang, J.; He, H.; Guo, X.; Wang, J.; Kou, Y. Application of parameter optimized variational mode decomposition method in fault diagnosis of gearbox. *IEEE Access* **2019**, *7*, 44817–44882. [[CrossRef](#)]
24. Ren, G.; Jia, J.; Mei, J.; Jia, X.; Han, J.; Wang, Y. An improved variational mode decomposition method and its application in diesel engine fault diagnosis. *J. Vibroeng.* **2018**, *20*, 2363–2378.
25. Sun, H.; Fang, L.; Zhao, F. A fault feature extraction method for single-channel signal of rotary machinery based on VMD and KICA. *J. Vibroeng.* **2019**, *21*, 370–383. [[CrossRef](#)]
26. Sun, G.; Jiang, P.; Xu, H.; Yu, S.; Guo, N.; Lin, G.; Wu, H. Outlier Detection and Correction for Monitoring Data of Water Quality Based on Improved VMD and LSSVM. *Complexity* **2019**, *2019*, 9643921. [[CrossRef](#)]
27. Hu, H.; Zhang, L.; Yan, H.; Bai, Y.; Wang, P. Denoising and Baseline Drift Removal Method of MEMS Hydrophone Signal Based on VMD and Wavelet Threshold Processing. *IEEE Access* **2019**, *7*, 59913–59922. [[CrossRef](#)]
28. Burges, C.J. A Tutorial on Support Vector Machines for Pattern Recognition. *Data Min. Knowl. Discov.* **1998**, *2*, 121–167. [[CrossRef](#)]
29. Hopfield, J.J. Neural networks and physical systems with emergent collective computational abilities. *Proc. Natl. Acad. Sci. USA* **1982**, *79*, 2554–2558. [[CrossRef](#)]
30. Chen, Z.; Zhao, F.; Zhou, J.; Huang, P.; Zhang, X. Fault Diagnosis of Loader Gearbox Based on an ICA and SVM Algorithm. *Int. J. Environ. Res. Public Health* **2019**, *16*, 4868. [[CrossRef](#)]
31. Ren, C.; An, N.; Wang, J.; Li, L.; Hu, B.; Shang, D. Optimal parameters selection for BP neural network based on particle swarm optimization: A case study of wind speed forecasting. *Knowl. Based Syst.* **2014**, *56*, 226–239. [[CrossRef](#)]
32. Nie, R.; Zhang, W.; Li, G.; Liu, X. A neural gust load alleviator for aircraft model using active control. In Proceedings of the 2009 IEEE International Conference on Intelligent Computing and Intelligent Systems, Shanghai, China, 20–22 November 2009; Volume 1, pp. 204–208.
33. Wang, S.; Zhang, N.; Wu, L.; Wang, Y. Wind speed forecasting based on the hybrid ensemble empirical mode decomposition and GA-BP neural network method. *Renew. Energy* **2016**, *94*, 629–636. [[CrossRef](#)]
34. Hinton, G.E.; Osindero, S.; Teh, Y.-W. A Fast Learning Algorithm for Deep Belief Nets. *Neural Comput.* **2006**, *18*, 1527–1554. [[CrossRef](#)] [[PubMed](#)]
35. Tamilselvan, P.; Wang, P. Failure diagnosis using deep belief learning based health state classification. *Reliab. Eng. Syst. Saf.* **2013**, *115*, 124–135. [[CrossRef](#)]
36. Zhu, H.Y.; Zhang, C.L.; Yue, X. Fault Diagnosis of Nuclear Power Equipment Based on HMM-SVM and Database Development. *Adv. Mater. Res.* **2010**, *139*, 2532–2536. [[CrossRef](#)]
37. Shen, Y.; Huang, Z. Performance Monitoring for Vehicle Suspension System via Fuzzy Positivistic C-Means Clustering Based on Accelerometer Measurements. *IEEE/ASME Trans. Mechatron.* **2015**, *20*, 2613–2620.
38. Yiakopoulos, C.; Gryllias, K.; Antoniadis, I. Rolling element bearing fault detection in industrial environments based on a K-means clustering approach. *Expert Syst. Appl.* **2011**, *38*, 2888–2911. [[CrossRef](#)]
39. Zhang, D.Q.; Chen, S.C. Clustering Incomplete Data Using Kernel-Based Fuzzy C-means Algorithm. *Neural Process. Lett.* **2003**, *18*, 155–162. [[CrossRef](#)]

40. Yugander, P.; Sheshagiri, B.J.; Sunanda, K.; Susmitha, E. Multiple kernel fuzzy C-means algorithm with ALS method for satellite and medical image segmentation. In Proceedings of the 2012 International Conference on Devices, Circuits and Systems (ICDCS), Coimbatore, India, 15–16 March 2012.
41. Yang, M.S.; Tsai, H.S. A Gaussian kernel-based fuzzy c-means algorithm with a spatial bias correction. *Pattern Recognit. Lett.* **2008**, *29*, 1713–1725. [[CrossRef](#)]
42. Liu, S.; Dong, L.; Liao, X.; Cao, X.; Wang, X. Photovoltaic Array Fault Diagnosis Based on Gaussian Kernel Fuzzy C-Means Clustering Algorithm. *Sensors* **2019**, *19*, 1520. [[CrossRef](#)]
43. Abdoos, A.A. A new intelligent method based on combination of VMD and ELM for short term wind power forecasting. *Neurocomputing* **2016**, *203*, 111–120. [[CrossRef](#)]
44. Liu, W.; Cao, S.; Chen, Y. Applications of variational mode decomposition in seismic time-frequency analysis. *IEEE J. Sel. Top. Appl. Earth Obs. Remote Sens.* **2017**, *9*, 3821–3831. [[CrossRef](#)]
45. Xiao, Q.; Li, J.; Bai, Z.; Sun, J.; Zhou, N.; Zeng, Z. A Small Leak Detection Method Based on VMD Adaptive De-Noiseing and Ambiguity Correlation Classification Intended for Natural Gas Pipelines. *Sensors* **2016**, *16*, 2116. [[CrossRef](#)] [[PubMed](#)]
46. Yan, X.; Jia, M.; Xiang, L. Compound fault diagnosis of rotating machinery based on OVMD and a 1.5-dimension envelope spectrum. *Meas. Sci. Technol.* **2016**, *27*, 075002. [[CrossRef](#)]
47. Hinton, G.E. A practical guide to training restricted boltzmann machines. In *Neural Networks: Tricks of the Trade*; Springer: Berlin/Heidelberg, Germany, 2012; pp. 599–619.



© 2020 by the authors. Licensee MDPI, Basel, Switzerland. This article is an open access article distributed under the terms and conditions of the Creative Commons Attribution (CC BY) license (<http://creativecommons.org/licenses/by/4.0/>).